Aircraft Automatic Flight Control System with Model Inversion

G. Allan Smith* and George Meyer†
NASA Ames Research Center, Moffett Field, California

An automatic flight control system concept is proposed for advanced aircraft configurations with severe nonlinear characteristics. A feature of the system is an inverse of the complete nonlinear aircraft force and moment model as part of the feed-forward control path. A method for the continuous real-time inversion of the aircraft model using a Newton-Raphson trim algorithm has been developed. The results of a simulation study of a vertical attitude takeoff and landing aircraft using the new inversion technique are presented. Maneuvers were successfully carried out in all directions in the vertical attitude hover mode. Transition runs showed satisfactory transient response from conventional flight through the region of lift curve slope reversal at an angle of attack of about 32 deg to hover at zero speed in the vertical attitude. Simulations were also conducted in conventional flight at high subsonic speed in steep climb and with turns up to 4 g. Successful flight tests of the system with the new model-inversion technique in a UH-1H helicopter have recently been carried out.

Introduction

SOME current high-performance fighter aircraft and helicopters, as well as many of those proposed for the future, have control and stability difficulties over some portions of their flight envelopes. These difficulties arise from highly nonlinear aerodynamic and propulsion characteristics, from undesirable coupling between axes, and from the extreme range of flight conditions encountered over the flight regime. There may be instances when automatic flight control will be desirable for these aircraft over at least portions of the flight regime. For example, precision trajectory control during night landing on a carrier at sea, terrain following with a helicopter, or hover mode control of a vertical attitude takeoff and landing (VATOL) aircraft; and, of course, complete automatic control is required for remotely piloted vehicles and cruise missiles.

A powerful new automatic flight control system concept suitable for trajectory control of the aforementioned aircraft types is being investigated at the NASA Ames Research Center. The implementation of this concept is made possible by an airborne digital computer. This is a total aircraft flight control system that combines attitude and thrust control in a unified system for operation over the full flight envelope.

The flight control system is based on a model-following concept in which several models of different complexity are used, including some that have essentially all of the aerodynamic and propulsion details that would be found in a complete model used for nonlinear, real-time, manual simulation studies. A unique feature of the control system is the continuous real-time inversion of such a complete nonlinear model of the aircraft for the purpose of defining the aerodynamic and propulsion control commands based on trajectory commands and regulator outputs.

The development of this control system concept is reported in Refs. 1-3. Successful flight tests in the augmentor wing jet STOL research aircraft,[4] DHC-6 aircraft,[5] and UH-1H helicopter[6] have been carried out. Simulator studies of a carrier landing were reported at the 1979 Digital Avionics Systems Conference,[7] a preliminary report of a simultion of hover-mode control for a VATOL configuration was given at the 1981 conference,[8] and a more complete report was made at the 1984 conference.[9] The overall structure of the control system is described in the above references, so only a brief explanation of the general system configuration will be presented here. Emphasis will be on a different technique for the real-time inversion of the nonlinear aircraft model and on a discussion of results of a simulation study of its application to control of a proposed VATOL aircraft over the full flight regime from vertical-attitude hover through the transition to conventional flight.

The simulation used the mathematical model of an advanced concept for a Navy VATOL aircraft configuration (tail sitter) suitable for launch and recovery at the side of a small ship. The aerodynamic and propulsion characteristics of this proposed aircraft were developed by the Vought Corporation.[10-12] This conceptual aircraft was chosen to illustrate the extensive flight regime and range of nonlinear characteristics that can be accommodated by the control system.

Some theoretical aspects of the mathematical basis for this control concept are included in Ref. 6 and some are mentioned briefly here in the conclusions. Theoretical studies are continuing and will be presented more fully in future publications.

The Control System Concept

The Ames control system concept has several key features. Fundamentally, it combines a feed-forward and feedback control, with the forward path split into a command section and a control section (Fig. 1). The feed-forward controller is shown in solid lines and the feedback control in dotted lines. Most symbols in this control system are three-dimensional column vectors with appropriate subscripts.

The feed-forward command section generates smooth, executable, and consistent acceleration A_c, velocity, V_c, and position R_c command vectors in the reference inertial axis system (north, east, and down) in response to corresponding rough trajectory command inputs A_i, V_i, and R_i. These rough inputs may be supplied from an air traffic control system, from ground vectoring, and/or from a trajectory time history stored in the computer or generated on line by the pilot using a side stick controller to command the trajectory accelerations.

The control section of the feed-forward controller computes the aircraft thrust and moment controls U needed to produce the total commanded acceleration vector A_T. It is a particular feature of the system that the series combination of the control section and the actual aircraft is essentially linear with

Presented as Paper 84-2627 at the AIAA/IEEE 6th Digital Avionics Conference, Baltimore, MD, Dec. 3-6, 1984; received May 12, 1986; revision received Oct. 17, 1986.

*Research Scientist. Associate Fellow AIAA.
†Research Scientist. Member AIAA.

decoupled axes when viewed from the command section. This is achieved by embedding an inverse of the aircraft force and moment model in the control section that determines the aircraft controls necessary to produce the commanded acceleration. The regulator feedback loop is closed around this approximate identity and hence can be easily designed by linear methods. It is called upon only to compensate for disturbances and model uncertainty.

Control System Implementation

The command generator (Fig. 1) accepts the rough trajectory commands that may not be executable because of discontinuities or deficiencies in some components of the vectors and produces a complete and consistent set of smooth, executable acceleration, velocity, and position vectors. This is accomplished by using a cannonical model of the aircraft; the model consists of a string of four integrators for each of the three channels corresponding to the components (north, east, down) of the input command vectors. Adjustment of the gains and limits provides smooth, executable output vector commands.[1] The smooth commanded acceleration (A_c) output of the command generator is added to the closed-loop feedback acceleration (ΔA_c) output of the regulator to give the total commanded acceleration vector (A_T).

Since the control section includes a complete nonlinear inverse model, it is appropriate to first consider the aircraft model itself (Fig. 2). This model has been specialized to represent the VATOL aircraft used in this simulation. The four controls (U) are normalized thrust and three angular acceleration controls for pitch, roll, and yaw that are converted to various aircraft control deflections. The VATOL jet engine has an output nozzle capable of swivelling through ± 15 deg in both pitch and yaw. The four input control commands are divided appropriately between the various aircraft controls, which include throttle, elevons, rudder, flaps, engine/nozzle angle, engine bleed-air reaction jets at the wing tips for roll control in the hover mode.

The outputs of the control actuators in Fig. 2 are input to the force and moment generating section, where the aerodynamic forces and moments in the body axes are computed as a result of angle of attack α and the velocity with respect to the wind-in-body axes V_{wb}. A detailed engine model with afterburner is used in the calculations of thrust and ram drag, including such refinements as engine gyroscopic moments and thrust losses caused by the nozzle turning angle and the bleed air used for roll control. The body axis moments M_b are used with the aircraft inertia matrix J and the Euler angular-rate equations to calculate angular acceleration $\dot{\omega}$, angular velocity, and aircraft attitude (which is expressed as TBR, the direction cosine matrix of rotation from the reference axes to the body axes). The inverse (transpose) TRB is used to transform F_b from the body axes to the reference axes. The addition of the gravity vector G and division by the aircraft mass m yields the acceleration vector A. This acceleration vector is the essential output of the direct model, although integrations to give velocity V and position R are included in Fig. 2.

The control section of the feed-forward controller (Fig. 1) is functionally the inverse of the aircraft force and moment model just described. The input is the total acceleration command vector A_T, which is applied to the model inverse to determine the corresponding thrust and attitude control positions. The overall operation of the trajectory control system should now be clear (through reference to the figures) and attention will be directed to the details of the model-inversion process, which differs substantially from the scheme used for previous applications of this concept.

The Model-Inversion Process

In the early implementations of this control system concept,[4,5] the model inversion was carried out with the aid of extensive tables of nonlinear aerodynamic data that related the lift and drag coefficients to the angle of attack and thrust. Simulation and flight results were satisfactory for these aircraft for which the configuration allowed the force and moment equations to be treated separately. An exhaustive search technique was then used to solve the two-dimensional tables.

The new model-inversion technique is suitable for more complex configurations with serious nonlinearities.

A symbolic explanation of the model-inversion scheme is presented in Fig. 3. Figure 3a indicates how the aircraft model shown in Fig. 2 is normally used in a conventional simulation study. For any particular set of linear and angular velocity

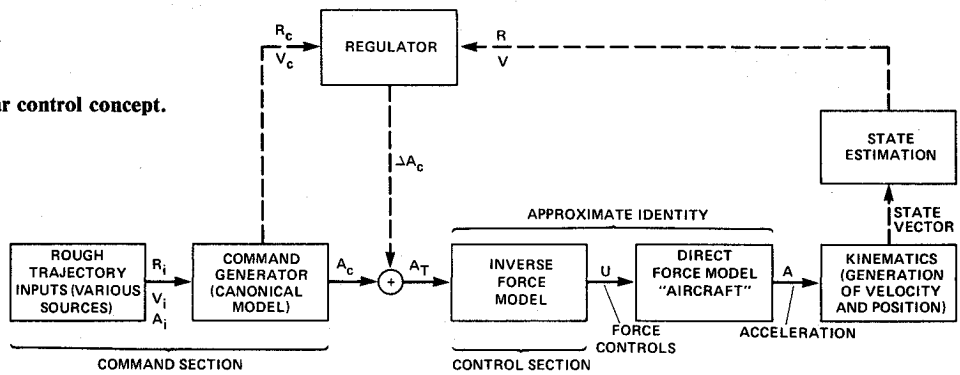

Fig. 1 Essential aspects of the nonlinear control concept.

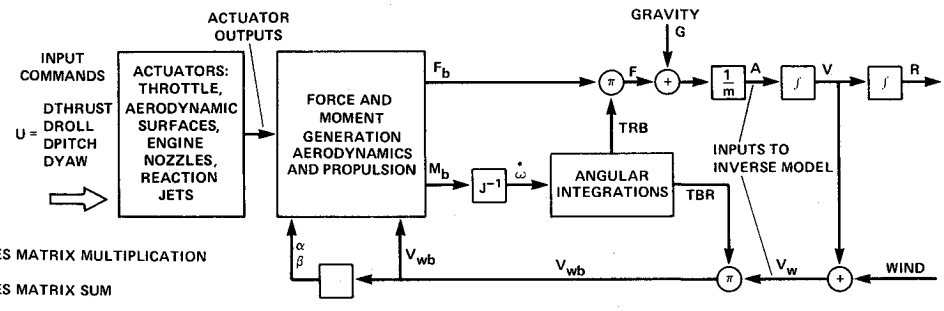

Fig. 2 Aircraft model.

vectors, knowledge of the control inputs U and the aircraft attitude TBR allows the output accelerations to be calculated by using equations for the various aerodynamic and propulsion forces and moments. The diagram in Fig. 3b represents the model-inversion problem. It will be recognized by those engaged in aircraft simulation studies as the approach for computing the control positions required to trim the aircraft at a given flight condition. The aircraft velocities and commanded accelerations and sideslip are specified as inputs and it is desired to calculate as outputs the corresponding aircraft attitude and controls that would produce the commanded inputs.

The inverse problem in Fig. 3b cannot be directly solved as illustrated, because we do not have analytical expressions for directly calculating the trim variables. Instead, the method applies an iterative Newton-Raphson trim procedure to the aircraft model of Fig. 3b. The Newton-Raphson trim is essentially a very refined cut-and-try process. It is a multivariable adapatation of Newton's method for finding the root of an equation by calculating a local derivative and using a linear extrapolation to find an approximation to the root in an iterative way.

The trim procedure is quite standard, so only a brief discussion of particular features will be given here. The trim procedure employs the force and moment vector equations in body axes:

$$F_b + TBR_c(G - mA_T) = EF$$

$$M_b + S(\omega_c)J\omega_c - J\dot{\omega}_c = EM$$

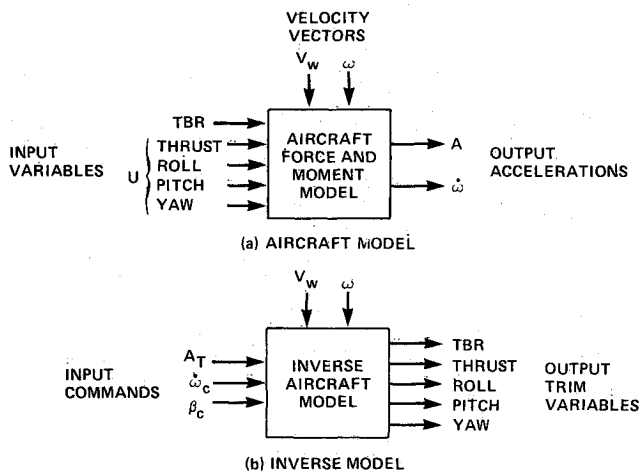

Fig. 3 Model inversion.

These equations apply to the aircraft model embedded in the control system and have, therefore, commanded variables as indicated by the subscript c. These two vector equations represent six scalar equations. The first three are force-error equations and the last three moment-error equations. The force represented in the body axes is F_b. The gravity vector G and the commanded acceleration vector A_T are both represented in reference axes. They are transformed by TRB_c so that all terms are in the body axes. If the aircraft model is in force trim, the three components of the error EF are zero. The M_b term is the torque vector represented in the body axes, ω_c the angular velocity, $\dot{\omega}_c$ the commanded angular acceleration, J the aircraft inertia matrix, and $S(\omega_c)$ the skew symmetric matrix function of angular velocity. If the model is in moment trim, the three components of EM are zero. For trim in conventional flight, the rotation matrix TBR_c is implemented as the product of five elementary direction-cosine matrices that represent heading ψ_c and flight path angle Γ_c defined by the commanded velocity vector V_c, a commanded sideslip β_c (usually zero), a roll angle ϕ_c, and an angle of attack α_c. The first three angles are fixed during a trim cycle; and roll and angle of attack are two of the trim variables. The other variables are the four controls U.

The trim procedure first selects trial values of the six trim variables (input variables in Fig. 3a). These are rough estimates for the initial trim—or values from the preceding trim cycle as the simulation proceeds. These trial trim variables are then used along with the commanded velocity vectors to calculate the resulting forces and moments, which are then substituted into the trim vector equations along with the commanded accelerations to find errors (EF and EM). If they are below specified tolerance values, the model is trimmed and the four trim variables that constitute the aircraft controls U are sent to the actual aircraft actuators. Nominal tolerances were taken as 0.001 g for the force equations and 0.005 rad/s^2 for the moment equations.

If any errors exceed their tolerance, a perturbation procedure is initiated. One trim variable is perturbed by a small amount from the trial value and the force and moment calculations are repeated to determine new values of the six trim equation errors. This is done six times, once for a perturbation of each of the six trim variables. A 6×6 Jacobian matrix of error derivatives of each scalar equation with respect to each trim variable is formed where, for example, the third-row fifth-column term is the partial derivative of the vertical force with respect to the angle of attack.

The Newton-Raphson procedure then inverts this matrix to give the estimated changes in the trial values of each trim variable to iteratively produce a set of balanced equations. These new trim variables are used to compute the forces,

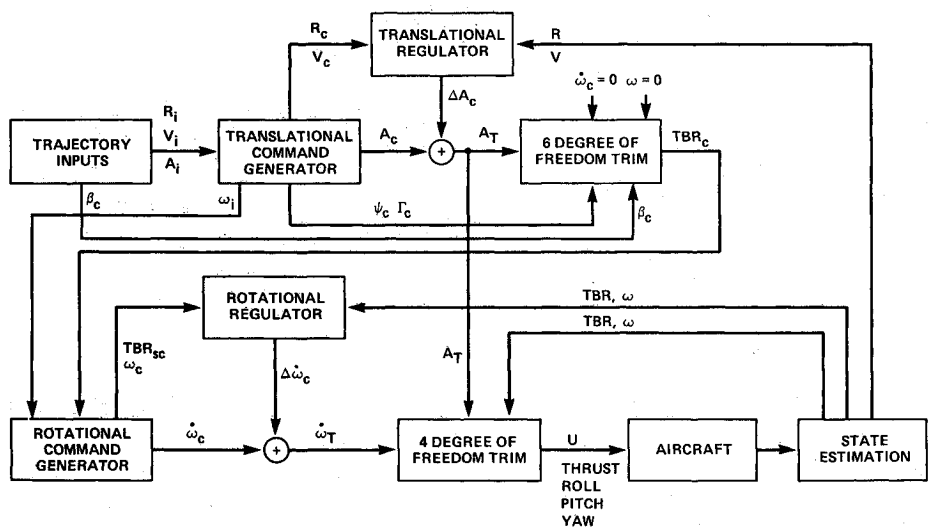

Fig. 4 Complete control system.

moments, and angular transformations required in the trim equations; if the six equation errors are less than the tolerance test, the model is trimmed. If not, the entire process is repeated with seven more passes through the model—one pass for each trim variable perturbation and one to verify trim. A single set of seven passes is sufficient for most flight conditions, but two or more sets are needed for parts of the trajectory when the commanded accelerations are changing rapidly or when external disturbances are encountered.

The use of the error equations in the trim procedure should now be clear. There are, however, several interesting details involved in the actual system. An important consideration arises when one attempts to trim the aircraft in a vertical attitude. When the aircraft is in a vertical attitude hover, all velocities may become zero, so that the angle of attack is undefined. Therefore, for low velocities in the vertical attitude, the angle of attack is replaced as a trim variable by the pitch attitude θ_c. Of course, α is still computed and used, although not as a trim variable, at all velocities where it is defined. Furthermore, in hover θ_c is nearly 90 deg with respect to the reference axes and is thus a singular point for the transformation TBR_c. Therefore, a change is made for low speed and the aircraft attitude is specified by the three conventional Euler angles; the angles are measured with respect to an inertial system rotated 90 deg from the reference axis system. This inertial system is called the perpendicular system and its axes are positive up, east, and north, respectively. For this condition, the transformation matrix from the perpendicular system to body axes is designated TBP_c and is implemented as the product of three elementary direction-cosine matrices representing the Euler angles. The pitch angle about the aircraft Y axis and the yaw angle about the z axis are taken as trim variables. The other Euler angle is a commanded heading angle about the vertical x axis; it is the angle between north and the aircraft landing gear in the vertical attitude and remains constant during a trim cycle.

A constant transformation matrix TPR is used to rotate from the references axes 90 deg about the east horizontal axis to the perpendicular system. These rotations are used in the force-error equations to get all terms in the perpendicular axis system so that the force-error equation becomes

$$TPB_cF_b + TPR(G - mA_T) = EF$$

In the simulation, a preselected pitch attitude of 60 deg from the horizontal was used to switch between the two different sets of force-error equations and to substitute the pitch attitude for the angle of attack as a trim variable. Operation was such that only very slight transients were observable in the system. This was expected, because the transfer is merely a computational operation and no switching of physical sensors is involved in an actual aircraft installation.

Other details in the trim procedure may be seen in Fig. 4, which is an overall flow diagram of the actual system. Note that several differences exist between it and the simplified configuration shown in Fig. 1. The control section has been split into translational and rotational sections, each with a command generator and a regulator. We have been discussing the six-degree-of-freedom trim whose input signal is the total commanded-acceleration vector A_T and whose output is the rough commanded attitude matrix TBR_c containing two of the trim variables. Furthermore, the angular velocity ω_c and angular acceleration $\dot{\omega}_c$ are taken as zero for the six-degree-of-freedom trim.

The matrix TBR_c is input to a rotational command generator that is functionally similar to the translational command generator and whose output, a smooth commanded angular acceleration vector $\dot{\omega}_{c_1}$, is combined with the output of the rotational regulator $\Delta\dot{\omega}_c$ to give a total commanded angular acceleration vector $\dot{\omega}_T$. The rotational regulator compares the aircraft attitude TBR and angular velocity ω with a smooth commanded attitude matrix TBR_{sc} and angular velocity ω_c to generate the closed-loop angular acceleration command increment. The total angular acceleration command is input to a four-degree-of-freedom Newton-Raphson trim section, which is entirely analagous to the previous six-degree-of-freedom trim section, except that only four trim equations are used: the three scalar moment equations and the first of the three force scalar equations.

The four trim variables are thrust, roll, pitch, and yaw. The actual aircraft attitude matrix TBR and angular velocity vector ω are used in these trim equations. The outputs of the four-degree-of-freedom trim are the four trim variables, which become the controls U and are input to the actual aircraft. This trim differs from the six-degree-of-freedom trim in that it has a commanded angular acceleration input and an angular velocity input in addition to the same commanded translational acceleration input A_T. The Newton-Raphson technique again requires one pass through the model to determine initial errors and four additional passes for perturbations of the four trim variables.

The simple diagram of Fig. 1 does not distinguish between the two trims. As shown in Fig. 4, the six-degree-of-freedom trim is used to determine aircraft attitude required for the commanded translational acceleration, but assumes zero angular velocity and acceleration. Two of the trim variables (angle of attack and roll angle) are used along with the commanded heading, flight path angle, and sideslip to determine the commanded attitude (pitch angle and roll angle along with the commanded heading for trim with the perpendicular referenced system). The four other trim variables for the six-degree-of-freedom trim are not used further. The four-degree-of-freedom trim uses the actual aircraft attitude and angular velocity and determines the four control variables necessary to produce the commanded angular acceleration vector. The four-degree-of-freedom trim switches from reference axes to perpendicular axes at the same time that the six-degree-of-freedom trim switches.

Simulation Results

A series of simulation studies was performed using the control system just described in the VATOL aircraft previously discussed. Maneuvers were first performed in the vertical-attitude hover mode in all directions, both individually and simultaneously and with various aircraft roll rates about the vertical axis. Accelerations up to 0.3 g and velocities up to 50 ft/s were investigated. The response to gusts and steady winds was also studied. Then in the conventional flight mode, major attention was directed to the transition between horizontal flight and hover. Tests were also carried out at high subsonic speed, with turns up to 4 g and flight path angles to 10 deg. The results of two different flight trajectories are presented: maneuvers in the vertical attitude at low speed and maneuvers during a transition run from conventional level flight to hover. Time histories are shown for each trajectory, including aircraft accelerations, velocities, and displacements as well as attitude angles and control variables.

The results shown are preliminary in that no particular effort was made to optimize the transient performance by gain or limit adjustments, since stable and reasonably satisfactory performance resulted from the initial settings.

Vertical-Attitude Maneuvering

Performance during maneuvers in the vertical attitude is shown in Fig. 5. Aircraft operation begins in hover in a vertical attitude at zero velocity with the landing gear facing north and the thrust equal to the aircraft's weight; the initial altitude was 1000 ft. A step command of 3 ft/s/s horizontal acceleration was applied at 3 s for a 15 s period, followed by a command of 3 ft/s/s acceleration vertically at 30 s for 10 s. A roll command of 20 deg/s about the vertical for 5 s was applied at 50 s. Thus, at 64 s, the aircraft was translating horizontally at 45 ft/s, translating up at 30 ft/s, and rolled to

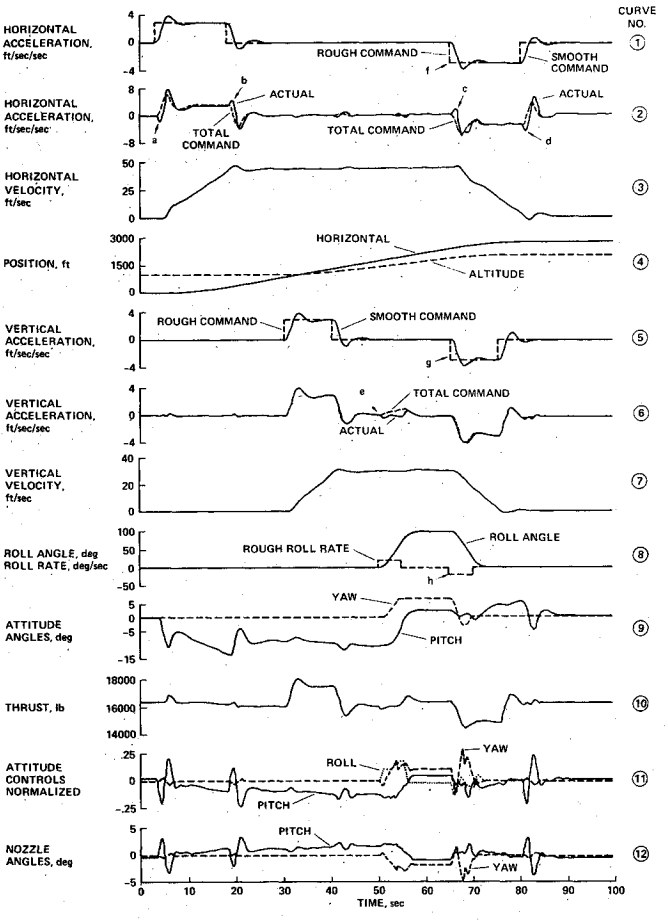

Fig. 5 Vertical attitude maneuvers about hover.

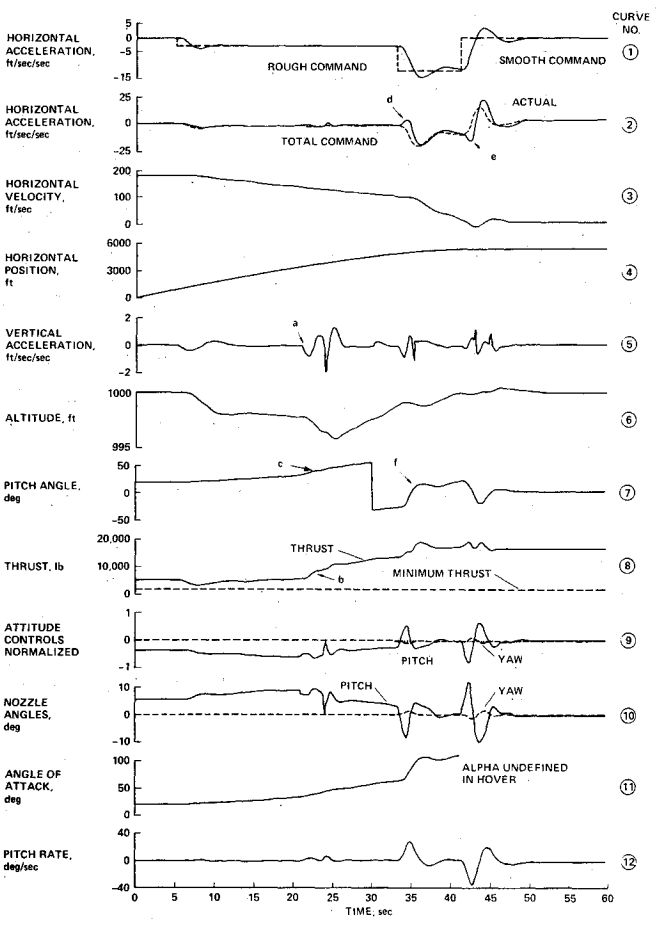

Fig. 6 Transition from forward flight to hover.

100 deg about the vertical axis. Simultaneous commands were then given to bring the aircraft back to the hover condition, which was essentially achieved by 90 s.

Curve 1 in Fig. 5 shows both the rough horizontal acceleration command $A_i(1)$, the first component of the rough commanded-acceleration column vector in Fig. 1, and the smooth command $A_c(1)$ from the command generator. The curve for $A_c(1)$ has appreciable overshoot, because the command generator forces its position and velocity outputs V_c and R_c in the steady state to be equal to the rough commanded inputs V_i and R_i, respectively. Hence, transient lags in the smooth velocity and position that are inherent in the basic aircraft must be compensated for by additional smooth commanded acceleration, even though the frequency response of the command generator canonical model is critically damped. The total commanded acceleration in curve 2 in Fig. 5 is $A_T(1)$ and includes the feedback corrective acceleration signal $\Delta A_c(1)$. The control system performance can be evaluated by noting how closely the actual acceleration $A(1)$, indicated by the solid line on the same plot, follows $A_T(1)$. The tracking is quite close except at the four points labeled a-d in Fig. 5, which show an initial aircraft acceleration in the direction opposite to the command. This reflects the nonminimum phase character (right half-plane zero) of the aircraft transfer function as the engine nozzle swivels forward to rotate the aircraft for translation and thus produces a momentary force opposing the intended translation. This is similar to the initial downward acceleration caused by elevator deflection when starting a climb in a conventional aircraft. In curve 3 of Fig. 5, the velocity reaches a steady value of 45 ft/s and the horizontal translation in curve 4 finally increases to almost 3000 ft.

Curves 5 and 6 of Fig. 5 show the vertical-acceleration commands and responses. There is no nonminimum phase effect in the vertical channel since the acceleration is due to engine thrust. The actual acceleration follows the total command very closely, except for a transient effect (point e in Fig. 5) during the roll-rate application. Curve 7 shows that vertical velocity responds with essentially no overshoot and reaches a value of 30 ft/s. The altitude response is shown along with horizontal distance on curve 4. Both the rough roll-rate command and the roll-angle response are shown on curve 8.

In the low-speed, vertical-attitude regime the aircraft attitude is measured by Euler angles in the perpendicular axis system. The pitch angle in curve 9 in Fig. 5 is not quite zero in hover, owing to an engine offset from the aircraft centerline. As shown in this plot, the aircraft pitches forward and the yaw angle remains zero until the aircraft starts to roll. Basically, the aircraft thrust vector is deflected to provide hoizontal acceleration; that is, a deflection from vertical of about 0.1 rad to give a forward acceleration of 0.1 g. No deflection would be required to sustain a constant velocity in the absence of aerodynamic forces. However, at an airspeed of 45 ft/s an aircraft pitch of 12 deg is needed to overcome the aerodynamic forces and engine ram drag effects. As the aircraft rotates about the vertical, the thrust vector is deflected in yaw and less in pitch until, after 100 deg of roll, there are about 6 deg of deflection in yaw and 2 deg in pitch. The size of the angles indicates the differences in the aerodynamic and propulsion forces on the two axes. During all of these commanded rotational maneuvers, the trajectory deviated less than 2 ft from the smooth command. The thrust curve in curve 10 shows the correlation with the vertical acceleration.

The normalized pitch channel signal in curve 11 of Fig. 5 reflects the pitching moment requirements needed for angular acceleration and counteraction of the aerodynamic moments as the airspeed increases. The yaw control indicates the shift from pitch to yaw control as the aircraft rolls. The roll control (shown by the dotted lines) initiates the roll rate at 50 s. Curve

12 shows the engine nozzle pitch and yaw deflections that remain well below their maximum limits of 15 deg.

At 64 s, simultaneous commands (points f-h in Fig. 5) are applied to all three axes to reverse the original commands and restore the aircraft to a hover condition at an altitude of 2000 ft. The commands and responses are nearly the inverse of the original, except for the coupling effects caused by the initial roll angle. It will be noted that the axes are quite well decoupled during separate commands of the first 50 s and that the major coupling effects for simultaneous commands occur in the controls and angular response such that, as a basic translational acceleration control system, the trajectory response in the different axes remains nearly decoupled for all commands. The trim equations were successfully iterated in one cycle for over 95% of the run and required only two computation cycles during the transient adjustments to the step commands.

Other vertical-attitude maneuvers showed similarly satisfactory response to lateral translational commands.

Translation Run from Forward Flight to Hover

Performance during a 60 s transition run at constant altitude is shown in Fig. 6. The aircraft is initialized in level flight at a velocity of 180 ft/s at an altitude of 1000 ft. A deceleration command of 3 ft/s/s is given at 5 s and is increased to 12 ft/s/s at 33 s. The commanded acceleration is reduced to zero at 41 s when the corresponding velocity command reaches zero. The vertical-acceleration command is zero throughout the run.

The point of particular interest in this run is the response during lift curve slope reversal beginning at about 22 s. The lift curve slope reversal near an angle of attack of 32 deg presents a problem to the essentially linear Newton-Raphson technique. In order to achieve trim, the predicted corrections were reduced to 80% to prevent hunting in the algorithm. The difficulty was compounded by the configuration with a large canard surface whose local angle of attack caused the slope of the lift curve for that surface to reverse at a different speed than for the main wing. Most of the same variables shown in Fig. 5 are also shown in Fig. 6, where they display many of the same correlations.

The step deceleration command $A_i(1)$ at 5 s shown in curve 1 of Fig. 6 results in the smooth command $A_c(1)$ on the same plot and the total command $A_T(1)$ and the aircraft response $A(1)$ on curve 2. The velocity V on curve 3 begins to decrease and the position R on the curve 4 continues to increase, but at a slower rate. A slight vertical-acceleration response occurs between 5 and 15 s accompanied by a 2 ft loss of altitude. The pitch angle and the angle of attack begin to increase from their initial values of 19 deg as the aircraft responds to the pitch control command in curve 9 and the corresponding pitch nozzle in curve 10. The thrust decreases almost to its minimum value during the initial deceleration.

As airspeed decreases, the angle of attack in curve 11 of Fig. 6 increases to maintain lift. The aerodynamic lift curve of the wing reaches its peak at an angle of attack of about 32 deg, at which point it reverses following wing stall. This effect is seen at 22 s where a vertical acceleration transient (point a) occurs as the trim process tries to obtain increased lift by increasing the angle of attack. At this point, the trim routine must maintain altitude by using additional engine thrust at a higher pitch attitude, shown by the thrust (point b) and pitch angle (point c) as the aircraft transitions to the vertical attitude mode. Airspeed is about 130 ft/s at this time. Only 5 ft of altitude were lost in the transition. The aircraft continues to slow down and the attitude increases until, at 30 s, a pitch attitude of 60 deg is reached and the attitude direction-cosine matrix is switched from the reference axis to the perpendicular axis system. This is seen in curve 7 of Fig. 6, where the pitch angle jumps from 60 to -30 deg. Only a slight response was observed in vertical acceleration. At 33 s, the deceleration command is increased to 12 ft/s/s and transients similar to those seen in Fig. 5 occur in all variables. The nonminimum phase behavior on the second plot is denoted by points d and e. The rapid rise to a vertical attitude (i.e., zero pitch angle) is shown by point f in curve 7 in Fig. 6. When the commanded velocity reaches zero, the deceleration command is removed and the aircraft comes to a hover position at zero velocity.

The transition starting at 22 s required two trim cycles for about 5 s and was equally troublesome when other transition runs were made going from low to high speed while climbing at 30 ft/s. There was less than 2 ft of sidewise deviation from the trajectory, except when wind gusts were applied. This aircraft has such a clean aerodynamic profile that deceleration along the flight path is difficult to achieve. An initial deceleration command of much more than 0.1 g would have called for a thrust from the trim process of less than the engine idle setting. The maximum deceleration obtainable varies from about 0.1 g at low speed to 0.4 g at an airspeed of 700 ft/s in conventional flight. Of course, much higher deceleration can be achieved in the vertical attitude mode.

Other Trajectories

Several other trajectories for which data are not shown were simulated. In particular, a turning, climbing, accelerating trajectory with a speed change of 300–900 ft/s and climb at a 10 deg flight path angle showed very satisfactory performance, including the execution of turns of 2, 3, and 4 g. Some trajectories were subjected to wind gusts and to initial offsets; the transient results were quite satisfactory.

Conclusions

The objective of this simulation study was to apply a recently developed trajectory control system concept to a vertical attitude takeoff and landing aircraft model with severe aerodynamic nonlinearities. Tests were carried out over an extensive flight envelope from vertical attitude hover through transition to conventional flight at high subsonic speeds. The control concept features the continuous real-time inversion of a detailed model of the aircraft. This study employed a new method of inverting the model by a Newton-Raphson trim technique instead of the inverse table look-up scheme usually used. Several specific comments regarding the study are:

1) The results presented here (and those of other simulation runs of different trajectories that were not presented because of lack of space) show that the control system performs satisfactorily over a large part of the flight envelope. The other tests included 4 g turns at Mach 0.8 and steep climbs as well as low-speed, vertical-attitude maneuvers in the hover mode with simultaneous velocity commands in all three axes and rapid rolling maneuvers.

2) The reversal in the lift curve slope near an angle of attack of 32 deg initially caused instability in the trim algorithm, but was overcome by minor modifications to the technique.

3) This investigation was undertaken to demonstrate the performance of the control concept with the Newton-Raphson model-inversion technique in a conceptual aircraft with a very large flight envelope. This objective was essentially accomplished, but a number of areas warrant study in greater detail to improve the performance and to define the limitations on maneuvering capability.

4) The use of a perpendicular inertial axis system for vertical-attitude hover maneuvers was quite satisfactory. No appreciable transients occurred, although the aircraft attitude matrix was simultaneously switched at three places in the control circuits. The switching point is not critical and can be anywhere between attitudes of 45 and 85 deg, so a suitable hysteresis loop can be designed to prevent any switching chatter when going through the switching region in either direction.

5) The system response to wind gusts (not shown here) was satisfactory for various reasonable combinations of wind magnitude and direction. However, trim failure could be induced for sufficiently severe disturbances. No attempt has yet been made to develop the logic to cope with such conditions.

6) The description of the control system concept mentioned that the rough trajectory command inputs can be generated on line by a pilot rather than by precomputed trajectory segments. Simulation runs were made for the conventional flight mode in which the pilot's fore-and-aft stick position commanded vertical velocity and the sideway stick displacement commanded the g level of a horizontal turn. Throttle position commanded airspeed. Under these conditions, the aircraft performance was quite satisfactory. It should be noted that only a few components of the rough commanded input vectors were thus generated and that some of these were in the body axis system or in a heading axis system rather than in the reference axis system. Nevertheless, suitable input transformations allowed the command generator to provide a full set of smooth commanded vectors in reference axes.

7) The credibility of these simulation results is supported by the flight test history of the concept in three aircraft. Flight tests in a DHC-6 Twin Otter aircraft[5] and in the augmentor wing jet STOL reasearch aircraft,[4] both of which used multidimensional table look-up for model inversion, showed good agreement between simulation and flight test results. A current flight test program using the Newton-Raphson model-inversion technique in a UH-1H helicopter has successfully controlled that aircraft over a complex maneuvering trajectory in spite of strong nonlinear coupling between axes.

8) The procedure described in this paper allows the construction of the complete state and control motions consistent with the a priori model of the aircraft state equation, whether or not the open-loop dynamics are stable, provided that the effects of right half-plane zeros are negligible. Whereas the necessary and sufficient conditions for linearizability are known in general, practical algorithms for transforming the state and control vectors when the system is not a strictly feedback one, have not been developed yet.

9) Flight envelope and control limits are conservatively imposed on the model motion by means of position and rate limiters. A more efficient switching logic is being investigated.

10) The extent to which the dynamics seen by the regulator are linearized and decoupled depends directly on the accuracy of the a priori model and the state estimation. For the cases investigated, the accuracy was such that the first-order effects of any nonlinearities were indeed removed. The resulting uncertainty in regulator dynamics was handled by standard robust regulator design techniques. However, the regulator design approach given here should not be used when large modeling errors are suspected.

11) The proposed algorithm may appear to require excessive computer capacity. In fact, that is not necessarily the case. For example, for the case of the UH-1H/VSTOLAND flight test, a Sperry-1819B flight computer was used. The sampling rate was 20 Hz. Of the 50 ms sampling interval, the complete algorithm took 20 ms. A new Jacobian (i.e., stability derivatives) matrix was available every 250 ms—that is, every fifth sample.

References

[1]Smith, G. A. and Meyer, G., "Application of the Concept of Dynamic Trim Control to Automatic Landing of Carrier Aircraft," NASA TP-1512, 1980.

[2]Meyer, G., "The Design of Exact Nonlinear Model Followers," *Proceedings of Joint Automatic Control Conference*, University of Virginia, Charlottesvile, June 1981.

[3]Meyer, G., "Nonlinear System Approach to Control System Design," NASA CP-2296, Hampton, VA, 1983.

[4]Meyer, G. and Cicolani, L. "Application of Nonlinear System Inverses to Automatic Flight Control Design-System Concepts and Flight Evaluations," *Theory and Applications of Optimal Control in Aerospace Systems,* AGARGograph 251, July 1981, pp. 10-1-10-29.

[5]Meyer, G. and Wherend, W., "DHC-6 Flight Tests of the Total Automatic Flight Control System (TAFCOS) Concept on a DHC-6 Twin Otter Aircraft," NASA TP-1513, 1980.

[6]Meyer, G., Hunt, R. L., and Su, R., "Design of a Helicopter Autopilot by Means of Linearizing Transformations," *Guidance and Control Panel 35th Symposium*, AGARD CP 321, 1983, pp. 4-1-4-11.

[7]Smith, G. A. and Meyer, G., "Total Aircraft Flight Control System-Balanced Open and Closed Loop Control with Dynamic Trim Maps," *Proceedings of IEEE/AIAA 3rd Digital Avionics Systems Conference*, Nov. 1979, p. 215.

[8]Smith, G. A. and Meyer, G., "Application of the Concept of Dynamic Trim Control and Nonlinear System Inverses to Automatic Control of a Vertical Attitude Takeoff and Landing Aircraft," *Proceedings of AIAA/IEEE 4th Digital Avionics Systems Conference*, Nov. 1981, p. 102.

[9]Smith, G. A. and Meyer, G., "Aircraft Automatic Digital Flight Control System with Inversion of the Model in the Feed Forward Path," *Proceedings of AIAA/IEEE 6th Digital Avionics Systems Conference*, Dec. 1984, p. 140.

[10]Driggers, H. R., "Study of Aerodynamic Technology for VSTOL Fighter/Attack Aircraft," NASA CR-152132, 1978.

[11]"USAF Stability and Control DATCOM," Air Force Flight Dynamics Laboratory, Wright-Patterson AFB, Ohio, Contract F33615-76-C3061, Oct. 1960 (April 1978 revision).

[12]Fortenbaugh, R. L., "A Mathematical Model for Vertical Attitude Takeoff and Landing (VATOL) Aircraft Simulation," Report prepared under Contract NAS2-10294 by Vought Corp. Dallas, for NASA Ames Research Center, Dec. 1980.